Modeling Agglomeration Processes in Fluid-Bed Granulation

Steven A. Cryer
Dow AgroSciences LLC, Indianapolis, IN 46268

Many agrochemicals are formulated as water dispersive granules through agglomeration, beginning with a fine powder (~ 1 μm) and ending with granules on the order of 500 μm. Powders are charged into a granulation system with a liquid binding agent, and granules are subsequently grown to an appropriate size. Granulation in fluid beds is presented using a mass conserving discretized population balance equation. Coalesce kernels governing the rate and extent of granulation are assumed dependent on the Stokes number, which is indirectly linked to important process variables (air and binder flow rate, bed charge, bed geometry) such that the physical processes governing particle coalescence and rebound are correlated to process variables. A new coalescence kernel is proposed based on physical insight, simplicity, and deterministic equivalent modeling to account for uncertainty. This kernel is based on a Stokes number method where uncertainty in the Stokes number is characterized by polynomial chaos expansions. The magnitude of the coalescence kernel is proportional to the probability of the distribution of Stokes number exceeding a critical value. This mechanistic/semiempirical approach to fluid-bed agglomeration fosters an environment for process scaleup by eliminating specific equipment and process variable constraints to focus on the underlying mechanisms for proper scale-up procedures. Model predictions using this new kernel are then compared to experimental pilot-plant observations.

Introduction

Granules and agglomeration

Granulation is the process of converting small diameter solid particles (typically powders) into larger diameter agglomerates made up of initial particles. A liquid binder solution (or water) is sprayed onto the powder to form a thin layer of liquid surrounding a particle. Liquid pendular bridges are formed as wetted particles coalescence. Pendular bridges subsequently form a crystallized structure once the water is evaporated off to yield a stable agglomerate. The particle is therefore "grown" from a smaller size into a larger agglomerate particle as measured by a mean particle volume or diameter.

A specific use for granulated material is in the formulation of agrochemicals and pharmaceuticals where often the end use product is a granule or pellet. Granules provide a defined quantity for dispensing in a premeasured package, eliminate dust, and are aesthetically pleasing for consumers. Granule porosity is such that dispersion in water can be maximized. Human exposure to pesticides is reduced through lowering contact exposure (dermal and inhalation). Water dispersion characteristics of granules dictate near liquid formulation performance in water (dispersion) for a solid material. Figure 1 illustrates an example of a commercial pesticide formulation for a Dow AgroSciences herbicide where agglomerated granules are the desired end product. The particles can be seen to exhibit a near spherical geometry with the major differences being particle size.

Examples of various types of process vessels used in granulation processes include pan, drum, and fluidized beds. The physical mechanisms involved in granulation for various equipment are similar; however, process variables and the effect these have on the agglomeration process can be dramatically different. Understanding the granulation process can aid in the ability to predict end point properties such as particle-

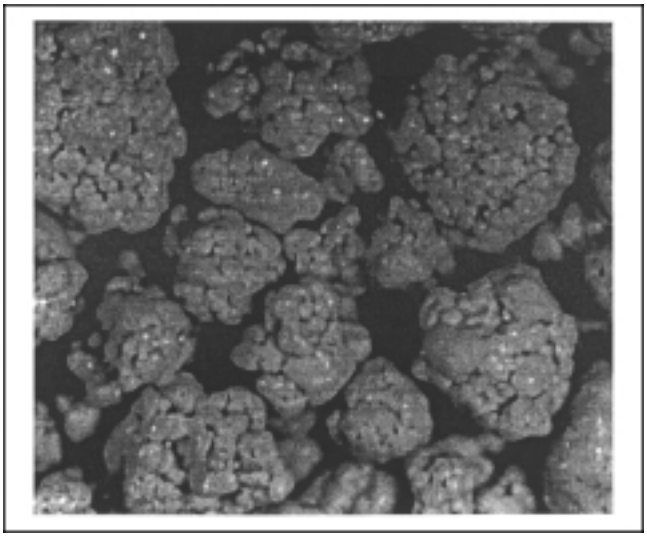

Figure 1. Enlargement (20×) of typical agricultural end use product.

size distribution, porosity, attrition strength, and dispersion characteristics in water.

Fluidized-Bed Granulation

The velocity of the fluidizing gas suspends the granules in the bed. The powder/granules are held within the granulater through filters at the top and a screen at the bottom. The suspended particles are free to collide and change properties as dictated by the physicochemical mechanisms involved. Both input feed (powder) and output product have associated attributes, but the size of the particle is the main attribute of interest for this analysis. Both initial particle and final product size are not single values but rather distributions of values. Thus, any predictive algorithm for simulating the behavior of granule growth must account for the nonuniformity of the initial particle-size distribution.

Optimization Requirements

Experimental observations for the batch fluid-bed system suggest that three granule size regimes occur during granulation. In Figure 2, particle size is plotted against the moisture content of the bed which is continually changing as atomized binder solution is added to the bed and evaporated off due to the fluidizing air volume. The first regime incorporates rapid granule growth as binder solution is added to the initially dry powder formulation. This is followed by the second regime which shows little granule growth for large changes in bed moisture. The final regime indicates rapid exponential like growth of granules for small changes in bed moisture. The operating regime where acceptable sized granules are formed occurs at or near the transition to the third regime where particle-size distribution can become very sensitive to operating conditions. Unacceptable large granules require re-milling which can alter the dispersion characteristics in water.

The greatest benefit towards optimizing the granulation process resides in understanding the coalescence and growth process for the granules in terms of process variables (that is, starting particle-size distribution (PSD), moisture and binder effects, air speed dependence on collision rate, and so on). Endpoints for optimization include reducing the overall final bed moisture content at the ending PSD such that equipment constraints are not exceeded and understanding the granule growth behavior near the granule optimal size regime.

Reduction of the number of runs where granule size is exceeded and optimal procedures for adding binder and increasing air-flow rate (currently a three-step process) can be accomplished through proper mechanistic elucidation of the granulation process. A net decrease in overall granulation cycle time and increase in throughput should ensue, along with a more aesthetically pleasing product as the oversized re-milled product is reduced.

Modeling the Granulation Process

Population balance

Conservation equations can be employed to understand the net processes involved in agglomeration because the mass of the starting powder is conserved. Tracking individual particle size (volume) as it grows is simply a statement of mass continuity. A population balance (PB) on particles can include kinetic expressions for each mechanism(s) responsible for changing a particle size. A PB follows the change in the granule size distribution as granules are born, die, grow, and enter or leave the control volume. Granules die when they coalesce with another granule to form a "new" granule with a new particle volume. Granules can grow through coalescence or through layering of binder material at the surface and can shrink through wear or attrition.

The PB equation is a nonlinear integropartial differential equation whose solution entails complex finite difference/element techniques due to the presence of the integral term. The additional computational load for solving such an equation limits its utility for engineering problems where real-time analysis is often sought for process control constraints. Numerical solutions to this continuity equation are CPU intensive but have been reported elsewhere (Dafniotis and Ray, 1996).

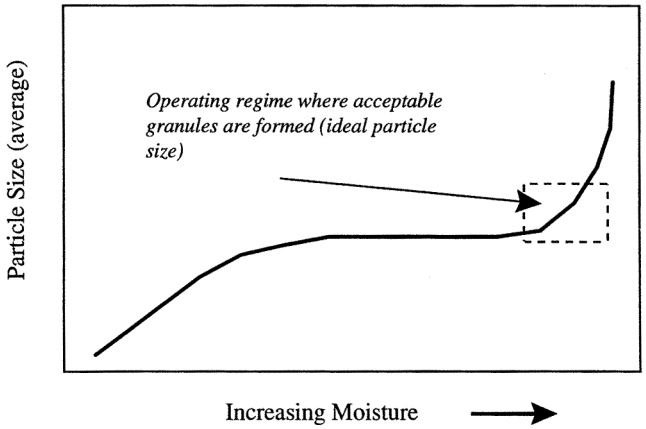

Figure 2. Empirical observations of fluid-bed granulation for several Dow AgroSciences herbicides.

Discretized Population Balance

The PB integro-partial differential equation can be approximated as a series of coupled nonlinear ordinary differential equations using appropriate simplifying assumptions (Hounslow et al., 1988; Lister et al., 1995). The approximation of a simplified version of the PB integrodifferential partial differential equation arises from the discretization of the particle-size volume over the volume space of interest. The particle volume discretization is given by

$$V_{i+1}/V_i = 2^{1/q} \tag{1}$$

which can also be expressed on a particle diameter basis assuming spherical particles. Here, V_i and V_{i+1} are the granule volumes for bin i and $i+1$, respectively. For example, if $q=1$, and the smallest particle size is 5 μm, then the volume discretization is given as 5, 10, 20, 40 and 80 μm and so on, as dictated by Eq. 1. Similarly, for $q=2$, the volume is discretized as 5, 7.07, 10.0 and 14.1 μm and so on. Thus, all particles within a PSD are uniquely binned into volume discretization intervals governed by Eq. 1 with mass continuity represented by Eqs. 2–3 (Lister et al., 1995). Particle volume space spans the smallest particle range for the starting powder up to the largest volume expected for an agglomerate granule

$$\begin{aligned}\left(\frac{dN_i}{dt}\right)_{\text{agg}} = &\sum_{j=1}^{i-S(q)-1} \beta_{i-1,j}N_{i-1}N_j\left\{\frac{2^{(j-i+1)/q}}{2^{1/q}-1}\right\} \\ &+ \sum_{k=2}^{q}\sum_{j=i-S(q-k+2)-k+1}^{i-S(q-k+1)-k} \beta_{i-k,j}N_{i-k}N_j \\ &\times\left\{\frac{2^{(j-i+1)/q}-1+2^{-(k-1)/q}}{2^{1/q}-1}\right\} + \frac{1}{2}\beta_{i-q,i-q}N_{i-q}^2 \\ &+ \sum_{k=2}^{q}\sum_{j=i-S(q-k+2)-k+2}^{i-S(q-k+1)-k+1} \beta_{i-k+1,j}N_{i-k+1}N_j \\ &\times\left\{\frac{-2^{(j-i)/q}+2^{1/q}-2^{-(k-1)/q}}{2^{1/q}-1}\right\} - \sum_{j=1}^{i-S(q)} \beta_{i,j}N_iN_j\frac{2^{(j-1)/q}}{2^{1/q}-1} \\ &- \sum_{j=i-S(q)+1}^{\infty} \beta_{i,j}N_iN_j \end{aligned} \tag{2}$$

$$s(q) = \sum_{p=1}^{q} p \tag{3}$$

Here, N_k represents the number density volume increment for bin k, and $\beta_{i,j}$ represents the coalescence kernel for two different discretized volume intervals. The coalescence kernel can be a scalar or a function of particle size. When $q=1$, Eq. 2 reduces to the original equation of Hounslow et al. (1988).

The coupled set of nonlinear ordinary differential equations (Eq. 2) is solved by fifth-order Runge-Kutta with monitoring of local truncation error and adaptive step size control.

Discretization of Particle-Size Distribution

Initial PSDs are typically measured from experimental observations and are required as input to the model. Current distribution types incorporated into the Dow AgroSciences modeling tool include exponential, normal, log-normal and any superposition of single mode distributions. The initial PSD of the starting powder must first be discretized based upon Eq. 1 and written as initial conditions for Eq. 2 for which ever distribution is chosen.

Figure 3 illustrates the effect of discretization on the initial PSD for q values of 1, 7 and 20. In all cases, the same normal distribution is assumed. It should be pointed out that as the value of q increases, the discretization step in volume is smaller. Thus, larger values of q will yield more accurate representations for PSD at the expense of computational efficiency. As q increases, the number of bin intervals (and thus ordinary differential equations) also increases for the same

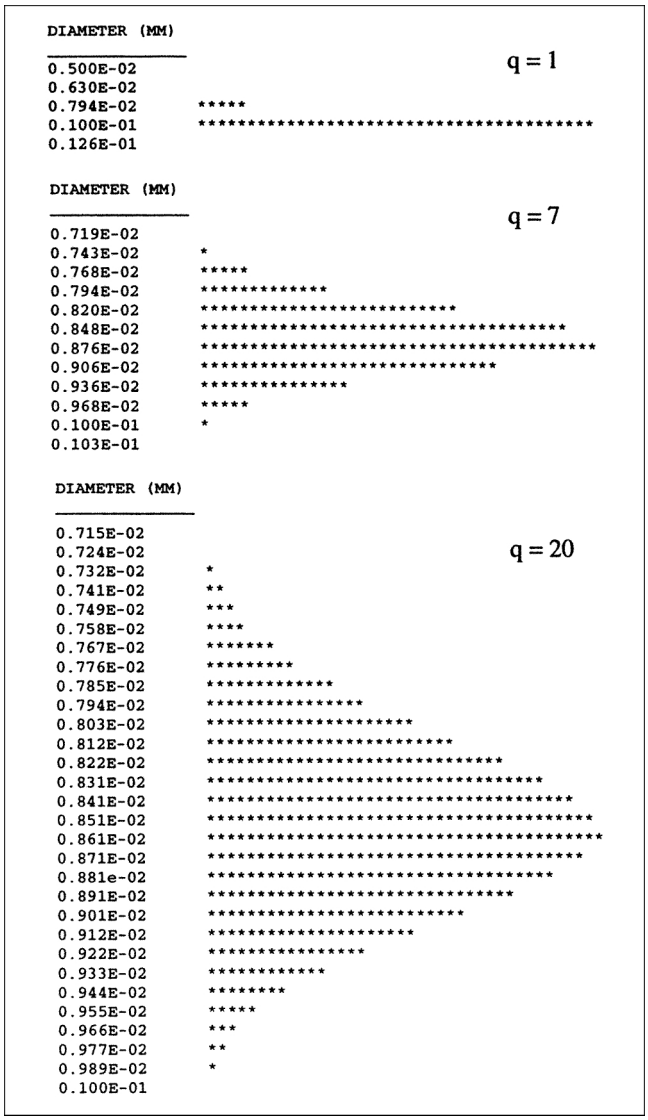

Figure 3. Accuracy of initial particle size (powder) distribution.

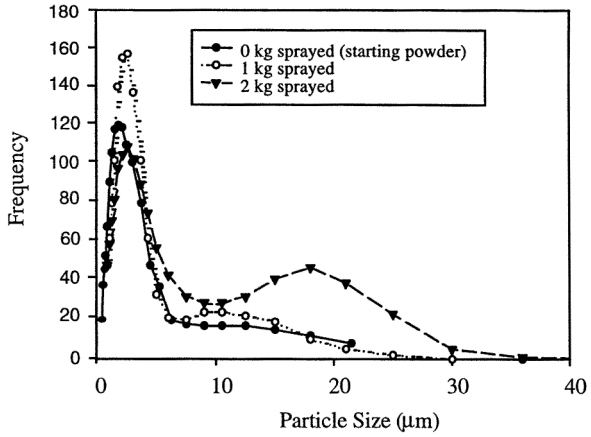

Figure 4. Changes in particle-size distributions during the "nucleation" regime.

volume range. Lister et al. (1995) have shown that computational requirements scale at approximately q^3.

Nucleation

Figure 4 represents an actual experimental run for the pilot-plant fluid-bed granulater of Dow AgroSciences. It is clear that a bimodal distribution does exist for small amounts of binder addition. The first single mode distribution represents the starting powder, and the second (growing) single mode distribution apparently is attributed to "nucleation" particle sizes based upon the size distribution of a surrounding droplet of binder solution.

As the agglomeration process proceeds in time, the bimodal distribution eventually coalesces into a single mode distribution as all of the powder is used up. Kinetic (empirical) modeling based upon experimental observations is used to describe the bimodal PSD early in the agglomeration process. It is assumed that the nucleation regime begins with the starting powder and is first observed when the bimodal distribution first forms. Single mode distributions representing the powder particle size and the atomizing binder droplets are superimposed to generate a "bimodal" distribution which is used as the starting particle size for the discretized population balance equation after a time delay.

Rates of formation for the bimodal distribution are based upon kinetic observations of experimental data. A nucleation routine is written to account for the behavior represented in Figure 4. The growth of the bimodal distribution is passed off as initial conditions for the population balance based upon observations as to when the "nucleation" particle sizes first begin to grow. This occurs at approximately 5 min into an experimental run.

Relationship of Agglomeration to Coalescence Kernel

Size-dependent coalescence kernel

The population balance is written in terms of a number distribution by volume because granule mass is conserved during the coalescence process. Coalescence is governed by the coalescence kernel or rate constant $\beta(u,v,t)$. Here, u and v are the different volumes for colliding particles, and t is time. The choice of kernel can dramatically affect the rate of coalescence and is typically a function of the granule size (through u and v dependence). These more complex kernels are often required to adequately represent experimental observations.

Proposed kernels

All proposed kernels are empirical or semi-empirical in nature and have been formulated largely based upon experimental observations. Coefficients in these kernels must be deduced through curve fitting to plant or laboratory data. A historical summary of proposed coalescence kernels is given in Table 1 (Ennis and Lister, 1997).

Physical Mechanism Descriptor Using Stokes Number

Coalescence of particles is analogous to chemical transformations for chemicals. Molecular interactions cause reactants to change structure, and the rate of change can often be approximated through kinetic modeling. Physicochemical interactions are responsible for agglomeration, and the extent of agglomeration of a species can be represented by a loss in number of particles (that is, population balance modeling). The proper design of processes involving agglomeration requires understanding and controlling physical mechanisms involved (both temporal and spatial), which are functions of initial conditions and process variables.

Figure 5 represents coalescence, the ultimate endpoint under consideration. Two particles or agglomerates come together with a certain inertia while simultaneously being wetted by the binder solution. Under certain conditions, the resulting collision will lead to coalescence, while, under other conditions, the particles will simply rebound.

Table 1. Proposed Size-Dependent Coalescence

Kernel	Reference
$\beta = \beta_0$	Kapur and Fuerstenau (1969)
$\beta = \beta_0 \dfrac{(u+v)^a}{(uv)^b}$	Kapur (1972)
$\beta = \beta_0 \dfrac{(u^{2/3}+v^{2/3})}{1/u+1/v}$	Sastry (1975)
$\beta = a(u+v)$	Golovin (1963)
$\beta = a\dfrac{(u-v)^2}{(u+v)}$	Golovin (1963)
$\beta = \begin{cases} k, & t < t_1 \\ \text{Golovin Kernel}, & t > t_1 \end{cases}$ k, t_1 constant, t_1 = transition time dictated by experimental observations	Adetayo et al. (1995)
$\beta = \begin{cases} k, & w < w^* \\ 0, & w > w^* \end{cases}$ k = constant where $w = \dfrac{(uv)^a}{(u+v)^b}$	Adetayo and Ennis (1997) w^* = critical granule volume at "cut off" a, b constants

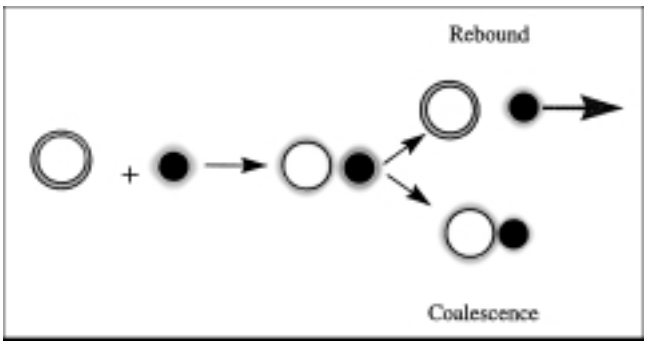

Figure 5. Conceptual model for granule consolidation where mechanistic understanding of coalescence and rebound is sought.

Ennis et al. (1990) proposed that the strength of the dynamic bridge, formed between colliding particles surrounded by a binder fluid, is an order of magnitude greater than the static force governed by the Laplace-Young equation. Thus, the strength of the dynamic liquid bridge governs the rate of granule consolidation while providing an explanation of the mechanism for coalescence. Coalescence occurs for colliding granules with insufficient relative kinetic energy to overcome the viscous dissipation force due to the surrounding binder fluid. A measure of the initial collisional kinetic energy to viscous dissipation can be given by the Stokes number (S_t)

$$S_t = \frac{4\rho U_c d}{9\mu} \tag{4}$$

where ρ is granule density, U_c is the relative collisional velocity, d is the average granule diameter, and μ is the solution phase binder viscosity.

μ and ρ are largely properties of the feed and binder solution. The collisional velocity is a function of both the type of granulation equipment and process variables which effect bed agitation.

Ennis et al. (1991) were the first to apply traditional coalescence theory to agglomeration characterization. These researchers proposed a methodology which could be used to qualitatively explain experimental observations of agglomeration. Clearly, for $S_t \gg 1$, the kinetic energy of the colliding particles dominates and thus the granules will not tend to coalesce. For $S_t \ll 1$, the viscous dissipation force of the binder fluid surrounding the granule is sufficient to dissipate the kinetic energy and coalescence will occur. From this reasoning, one can conclude that there exists a critical Stokes number (S_t^*) below which coalescence will occur and above which coalescence will not occur. The transition between colliding particles coalescing or rebounding is given by S_t^*. Particles colliding with $S_t > S_t^*$ suggest inertia dominates and the particles will rebound. Similarly, for collisions where $S_t < S_t^*$, the particles will coalesce as the momentum transfer at the collision is dissipated by the viscous action of the binder surrounding the granule. S_t^* can generally be determined by experiment or calculated from experiments with different granule properties (Tardos, 1995).

Successful coalescence requires that $S_t < S_t^*$. Theory provided by Barnocky and Davis (1988) for the collision of two rigid granules coated by a viscous layer provide a theoretical basis for determining S_t^*.

Both S_t and S_t^* are dynamic numbers since parameters change throughout the granulation process. Distributions for U_c and d occur throughout the fluid bed at any given time. Using the Stokes number analogy, Ennis et al. (1991) could explain experimental observations where rapid growth was followed by a much slower growth rate. The fast growth rates were attributed to noninertial granulation where the particle Stokes number is less than the critical value, while the slower growth regime was attributed to particle Stokes numbers above the critical value. Control of granule growth and consolidation for all types of granulation processes can only be achieved through proper correlation of the coalescence kernel with operational parameters. The Stokes number theory provides a physical basis for use in any correlation procedure.

Relating coalescence kernel to process variables

The key to successful modeling of the fluid-bed granulation process arises in relating the internal Stokes number to process variables. Parameters in the Stokes number which are not constant are the particle diameter and collision velocity. The discretized population balance model calculates the particle-size distribution as a function of time for a given kernel approximation. Thus, an approximation for the collision velocity between particles must be deduced before the Stokes number can be determined. The remainder of this section is devoted to summarizing simple algorithms for describing the transient distribution of Stokes numbers within a fluid-bed granulater. Particle coalescence and rebound can be calculated once the distribution of Stokes numbers is determined at a given point in time. The relative ratio of coalescence to rebound represents the rate of agglomeration as a function of time.

Particle Collision Velocity

One variable required in the Stokes number analysis is the particle collisional velocity (U_c). Ennis et al. (1991) provided an order of magnitude analysis for estimating the collisional velocity of particles in a fluid-bed system.

$$U_c \sim \frac{12 U_b a}{\bar{d}_b} \tag{5}$$

where U_b is the gas bubble rise velocity, a is the granule radius, and $\bar{d}_b$ is the average gas bubble diameter.

Fluid-bed observations are often thought of as analogous to a boiling liquid, because once a bed is fluidized, increases in the superficial velocity creates gas flow through the bed which can cause spouting and two-phase flow dynamics. Gas bubbling through the fluid bed is characterized by the gas bubble velocity (U_B) and gas bubble diameter ($\bar{d}_b$). A simple procedure is needed to estimate U_B and $\bar{d}_b$ which can subsequently be used in Eq. 5 for an estimate of the collisional velocity (U_c). The Stokes number and granulation regime can be characterized once U_c is known.

Gas Bubble Velocity

The collision velocity of agglomerates should be correlated against process variables since the collisional velocity is a sensitive parameter in the Stokes number analysis. In the absence of such data, one can resort to existing fluid-bed correlations that describe both bubble formation, growth, and rise velocity. It is assumed that the density of the agglomerates remains constant as they grow in size. In this way, the transition between different Geldart classification regimes based upon size alone can be easily followed. The population balance model calculates the number of particles and the particle-size distribution within the granulator at any given time. A volume median diameter is used as a representative particle size in various correlations that have been developed for different Geldart classification schemes to describe bubble growth and rise velocity. Correlations used in the fluid-bed model are given by Eqs. 6–14.

The minimal fluidization velocity is determined by Eqs. 6–7 for coarse and fine particles (Kunii and Levenspiel, 1991).
Coarse Particles

$$\frac{d_p U_{mf} \rho_g}{\mu} = \left[(28.7)^2 + 0.0494 \left(\frac{d_p^3 \rho_g (\rho_s - \rho_g) g}{\mu^2} \right) \right]^{1/2} - 28.7 \tag{6}$$

Fine Particles

$$\frac{d_p U_{mf} \rho_g}{\mu} = \left[(33.7)^2 + 0.04084 \left(\frac{d_p^3 \rho_g (\rho_s - \rho_g) g}{\mu^2} \right) \right]^{1/2} - 33.7 \tag{7}$$

where U_{mf} is the superficial gas velocity at minimum fluidizing conditions (m/s), ρ_g is the density of gas, ρ_s is the density of solid, d_p is the particle diameter, and μ is the viscosity of gas.

Bubble size

Bubble size is a function of bed height and the type of distributor plate in the fluid bed. The initial bubble diameter (d_{bo}) leaving the distributor plate is given by (Kunii and Levenspiel, 1991).
For lower flow rates

$$d_{bo} = \frac{1.30}{g^{0.2}} \left[\frac{U_o - U_{mf}}{N_{or}} \right]^{0.4} \tag{8}$$

or

$$d_{bo} = \frac{2.78}{g} (U_o - U_{mf}). \tag{9}$$

For higher flow rates. Here U_o is the superficial gas velocity (m/s) and N_{or} is the number of orifices per unit area of distributor (m^{-2}).

The value calculated from Eq. 8 cannot exceed that calculated from the high flow rate correlation (Eq. 9). These correlations assume a triangular array of orifices for the distributor plate. Similar correlations would have to be used for other types of distributor plates.

The bubble size as a function of bed height is estimated by the correlation proposed by Mori and Wen (1975) where an expected bubble diameter of limited size (d_{bm}) is given as

$$d_{bm} = 0.65 \left[\frac{\pi}{4} d_t^2 (U_o - U_{mf}) \right]^{0.4} \tag{10}$$

and the bubble size as a function of bed height is given by

$$\frac{d_{bm} - d_b}{d_{bm} - d_{bo}} = \exp\left(-0.3 \frac{z}{d_t} \right) \tag{11}$$

where z is the height in the bed (m), and d_t is the bed diameter (m).

Fluid beds on a manufacturing scale are often operated at a fixed height (L_{bed}). As the particles grow in size, the superficial velocity is increased to keep the bed height constant. Thus, an average bubble diameter within the bed can be estimated by integrating Eq. 11 over L_{bed} to yield an average bubble diameter ($\bar{d}_b$) of

$$\bar{d}_b = d_{bm} - \frac{(d_{bm} - d_{bo}) d_t}{3 L_{\text{bed}}} \left\{ \exp\left(- \frac{3 L_{\text{bed}}}{d_t} \right) - 1 \right\} \tag{12}$$

This bubble diameter is used in the following correlations for determining the bubble rise velocity.

Bubble rise velocity

The rise velocity is a function of the Geldart solids classification. An appropriate correlation is chosen to estimate bubble rise velocity that spans particle sizes from Geldart A to D (Werther, 1978)

$$U_b = \psi (U_o - U_{mf}) + \alpha U_{br} \tag{13}$$

where ψ is the fraction of visible bubbles, α is the factor to account for the deviation of bed bubbles from single rising bubbles, and U_{br} is the bubble rise velocity for a single bubble.

Based on a simple two-phase theory, Davidson and Harrison (1963) proposed U_{br} which can be represented as

$$U_{br} = 0.711 (g d_b)^{1/2} \tag{14}$$

Values for ψ are curve fit to data of Werther for Geldart A, B, and D solids. In addition, values for α have been proposed by Werther.

A representative bubble rise velocity can now be estimated using Eqs. 13–14. Both U_b and $\bar{d}_b$ are used with Eq. 5 to yield an estimate of the particle collision velocity (U_c) at each time step in the simulation.

Stokes Number Determination Under Uncertainty

The Stokes number can now be determined since the particle collision velocity can be estimated as described in the pre-

vious sections. The deterministic equivalent modeling method (Tatang, 1995) is used to account for uncertainty in independent parameters in the Stokes number. The deterministic equivalent modeling method represents uncertain inputs and outputs of a model as polynomials of random variables.

A polynomial chaos expansion is a weighted sum of orthonormal polynomials in standard normal random variables. The orthogonal polynomials are the Hermite polynomials which for a one-dimensional polynomial chaos expansion for a parameter a_i, can be represented by Eq. 15

$$a_i = a_{i0} + a_{i1}\,\xi_i + a_{i2}\left(\xi_i^2 - 1\right) + a_{i3}\left(\xi_i^3 - 3\xi_i\right) + a_{i4}\left(\xi_i^4 - 6\xi_i^2 + 3\right) + \ldots \quad (15)$$

where the standard normal variable ξ_i has the probability density

$$f_\xi(\xi_i) = \frac{1}{\sqrt{2\pi}} \exp\left(\frac{-\xi_i^2}{2}\right). \quad (16)$$

The terms 1, ξ_i, $\xi_i^2 - 1$, $\xi_i^3 - 3\xi_i$, $\xi_i^4 - 6\xi_i^2 + 3$ are the first five orthonormal polynomials with respect to the standard normal distribution.

For orthonormality, if the inner product of two polynomials $p_j(\xi)$ and $p_k(\xi)$ is defined as

$$\left(p_j(\xi), p_k(\xi)\right) = \int_{-\infty}^{\infty} p_j(\xi)\,p_k(\xi)\,f_\xi(\xi)\,d\xi \quad (17)$$

then the orthonormality implies that

$$\left(p_j(\xi), p_k(\xi)\right) = \begin{cases} 1 & \text{if } j = k \\ 0 & \text{if } j \neq k \end{cases} \quad (18)$$

The coefficients, a_{i0}, a_{i1}, a_{i2}, a_{i3}, a_{i4}, … in Eq. 15 are constants determined by the distribution for the parameter a_i. If a_i is normally distributed with mean μ_i and standard deviation σ_i, then

$$\begin{aligned} a_{i0} &= \mu_i \\ a_{i1} &= \sigma_i \\ a_{ij} &= 0 \ (\text{for } j \leq 2) \end{aligned} \quad (19)$$

Particle diameter and collisional velocity are approximated using polynomial chaos expansions and are substituted into the expression for the Stokes number to create a stochastic model. The residual of the stochastic model is made orthogonal to the basis functions (that is, 1, ξ_1, and ξ_2 for this example) and transformed into a set of deterministic equivalent equations using a variational approach by Galerkin (Ghanem and Spanos, 1991). ξ_1 and ξ_2 are independent random variables represented by Gaussian distributions.

It is assumed the particle collision velocity is normally distributed since the particle velocity is only an estimate. The deterministic equivalent modeling method approach can be easily extended to higher-order terms to account for additional moments should non-normal behavior be observed.

The collisional velocity (U_c) and granule diameter (d) used in Eq. 4 are approximated as second-order polynomial chaos expansions represented as

$$U_c = U_o + U_1\,\xi_1 \quad (20)$$

$$d = d_o + d_1\,\xi_2 \quad (21)$$

where U_o, d_o, and U_1, d_1 are the mean and standard deviations for the collision velocity and particle diameter, respectively. Higher-order terms in a chaos expansion represent higher-order moments in the distribution. The dependent variable (Stokes number) is also expanded in terms of the independent random variables to first order.

$$S_t = St_o + St_1\,\xi_1 + St_2\,\xi_2 \quad (22)$$

Substituting Eqs. 20–22 into Eq. 4, and applying Galerkin principles to impose normality (Ghanem and Spanos, 1991; Tatang, 1995) yields the coefficients of S_{to}, S_{t1}, and S_{t2} for Eq. 22

$$S_t = \frac{4\rho}{9\mu}\left(U_o d_o + U_1 d_o\,\xi_1 + U_o d_1\,\xi_2\right). \quad (23)$$

Estimates for U_c (Eq. 20) are made as follows. It is known that velocity scales linearly with pressure gradients for incompressible flows. In the fluid bed, the pressure drop across the column is measured and the length of the column is a constant. A mean and standard deviation for pressure drop can be derived from transient experimental observations. The percent deviation from the mean pressure drop is indicative of the percent deviation from the collisional velocity mean via the linear scaling of pressure and velocity. This scaling relationship used to estimate the granule collision velocity variance is given by Eq. 24.

$$U_1 \sim U_o \frac{\Delta P_{\text{ave}}}{\Delta P_{\text{Stdev}}} \quad (24)$$

ΔP_{ave} is the pressure drop average across the bed (calculated from experimental observations), and ΔP_{Stdev} is the pressure drop standard deviation across the bed (calculated from experimental observations).

Figure 6 compares Eq. 23 to the Monte Carlo solution (1,000 iterations) of Eq. 4 assuming both the collision velocity (mean = 10 cm/s, standard deviation = 4 cm/s) and particle diameter (mean = 0.004 cm, standard deviation = 0.001 cm) are normally distributed. Particle density was assumed to be 1.0 g/cm^3, while the viscosity of the binder liquid (μ) is assumed that of water (0.01 g/cm s). Equation 23 is incorporated into the modeling system to account for uncertainty in calculated parameters that affect the Stokes number magnitude and associated uncertainty.

A Stokes number distribution is calculated at each numerical time step since both the particle-size distribution and collision velocity are functions of time. Figure 7 qualitatively illustrates the granulation regimes with respect to the Stokes number (S_t) and critical Stokes number (S_t^*). Cumulative

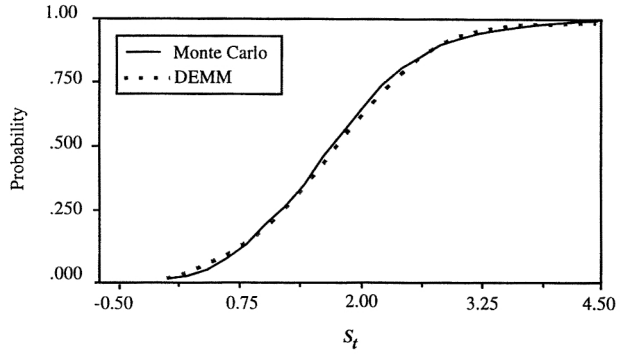

Figure 6. Comparison between the deterministic equivalent modeling method and Monte Carlo for Stokes number uncertainty.

particle-size distributions are plotted as a function of time. Regions 1–2 are characteristic of the noninertial regime since the Stokes number distribution within the fluid bed is less than S_t^*. Regions 3–4 represent the inertial regime where the amount of collisions resulting in coalescence is proportional to the probability of Stokes numbers less than S_t^*. Region 5 represents the coating regime since all Stokes numbers are greater than S_t^* and thus all collisions will result in rebound since growth can only occur through layering of the binder material.

A new empirical coalescence kernel (β) is postulated to represent the quantitative behavior of Figure 7 for S_t and S_t^* and is given by Eq. 25

$$\beta = \beta_o \int_{-\infty}^{S_t^*} f(\phi, t)\, d\phi \tag{25}$$

where $f(\phi, t)$ is the discrete probability density function for the Stokes number, and β_o is the constant determined from experimental data.

This kernel has many advantages over previously proposed kernels. Advantages include (1) simplicity, (2) physically based on Stokes number methodology, (3) it is easily incorporated into a numerical modeling procedure, (4) it accounts for uncertainty in parameter predictions/calculations, and (5) it can model similar behavior of other proposed kernels with less "free parameters." Coalescence is a function of particle size,

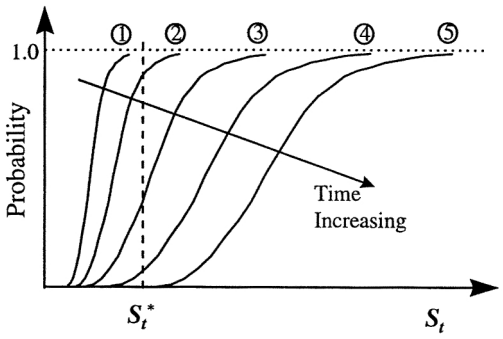

Figure 7. Qualitative representation of Stokes number Kernel used in population balance modeling.

collision velocity and physical properties of the fluid since the kernel is dependent upon the Stokes number. The collisional velocity is a function of the process variables specific for the fluid bed of interest.

Accounting for Nonlinear Agglomeration Near Particle Optimal Size

The kernel represented by Eq. 25, and those postulated by other researchers (Table 1), cannot describe the rapid exponential growth near the optimal particle size as qualitatively represented in Figure 2. This region of rapid growth immediately following a regime of slow growth has been observed in both pilot- and manufacture-scale fluid-bed granulaters of Dow AgroSciences LLC.

The coalescence kernel decreases as the simulation is increased from time 0 (and particles are growing), which results in a reduction of agglomeration with time. This apparently occurs over the majority of the operation times for the fluid bed for many of the Dow AgroSciences experimental observations. This behavior suggests that S_t^* is not a constant, but rather varies within the experimental time frame. Thus, S_t^* is treated as a free parameter which can be assumed to be characterized by Eq. 26 (or some other approximation). Equation 26 illustrates a function where S_t^* increases with time, and the percentage of collisions resulting in coalescence can also increase. Coefficients in Eq. 26 can be determined based upon comparison to experimental observations

$$S_t^* = \alpha_1(1 + e^{t-\alpha 2}) \tag{26}$$

If a functional form representing the time dependence of the critical Stokes number is used (such as Eqs. 25–26), then three free parameters are required to fully characterize the coalesce kernel behavior over the entire fluid-bed response surface. These coefficients, α_1, α_2, and β_o, can be determined through comparison between model predictions and experimental observations. S_t^* can either increase or decrease with time depending upon the sign and magnitude of α_2.

This proposed kernel now has as many free parameters as other proposed kernels (three) but is far more versatile. The versatility arises from the physical basis (Stokes number) where process variables can be directly accounted for, and the ability to simulate the rapid topology changes in response to surface output (Figure 2) seen experimentally. This latter observation cannot be accommodated using other proposed kernels. If α_2 is greater than the time scale of the experiment, then S_t^* remains constant through out time.

Model Results

Figure 8 illustrates the probability of exceeding S_t^* throughout the simulation process. It is clear that this probability varies with time. Only in the limit of $S_t^* \rightarrow$ infinity will the probability of $S_t < S_t^*$ be a constant (that is, probability $S_t < S_t^* = 1.00$). For small values of S_t^*, the probability of $S_t < S_t^*$ decreases rapidly which would be indicative of a regime where particles only rebounded.

A representative example of pilot-plant process variables used as input for the modeling system can be seen in Figure

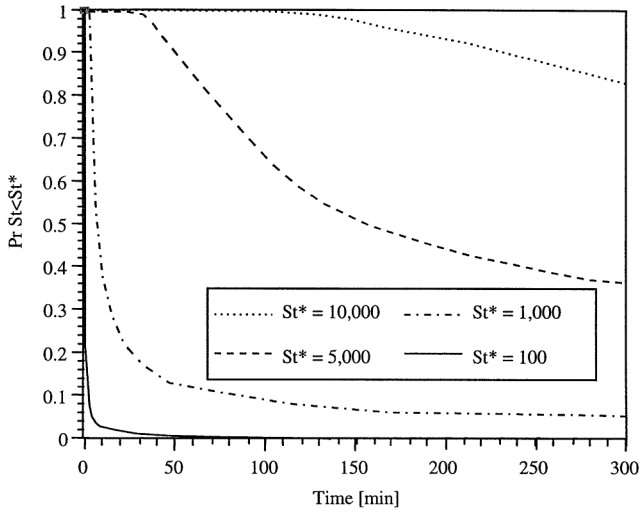

Figure 8. Representative probability of exceeding the critical Stokes number as a function of critical Stokes number (S_t^*) for two-parameter kernel ($\alpha_2 \gg t$).

9. Experimental observations, with model predictions, from a single fluid bed run using the process variables of Figure 9 are seen in Figure 10. The three-parameter kernel (α_1, α_2 finite, β_0) is superior to the two-parameter kernel (α_1, $\alpha_2 \gg t$, β_0) for such data sets where multiple growth regimes are

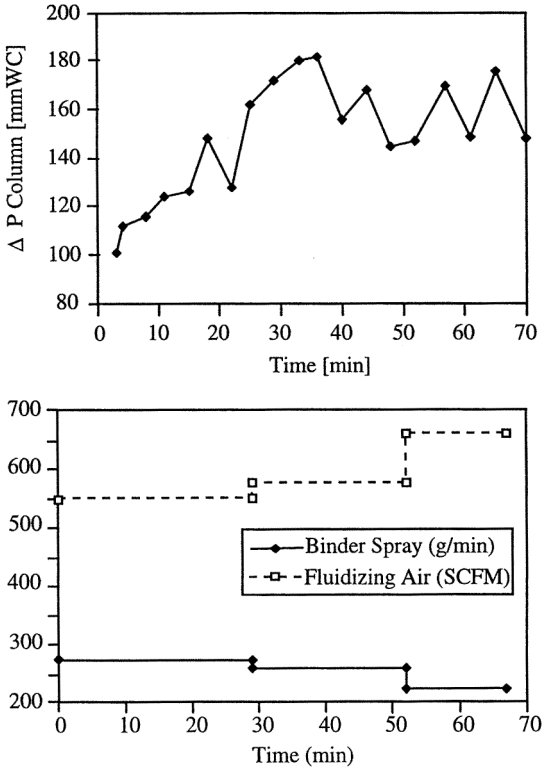

Figure 9. Representative process variables measured from a single experimental run of a pilot-scale fluid-bed granulater.

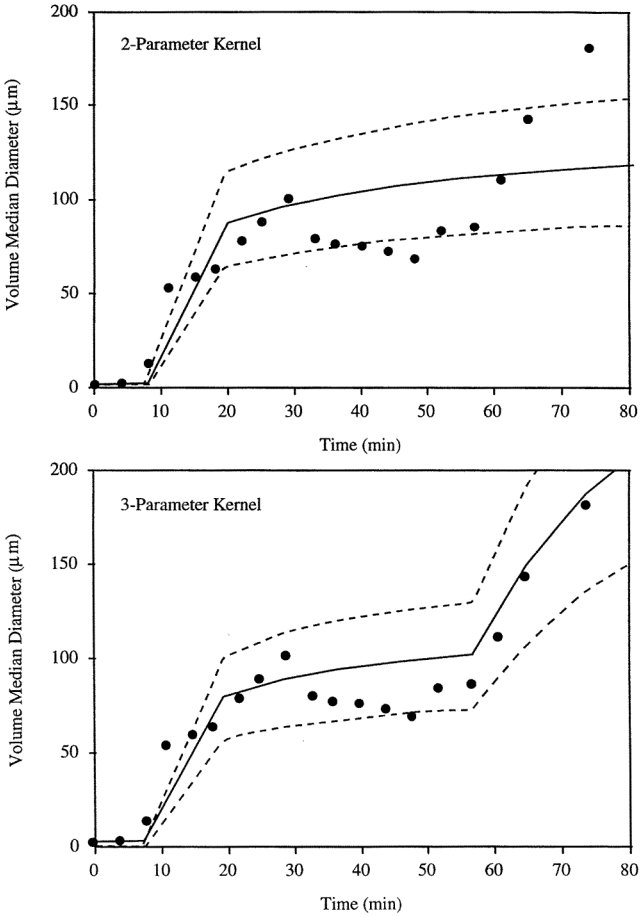

Figure 10. Comparison between two- and three-parameter kernel model predictions (with 50% confidence interval) against pilot-plant observations.

encountered throughout the granulation process. Figure 11 represents experimental results under different process conditions to illustrate the capabilities of the DPB system to

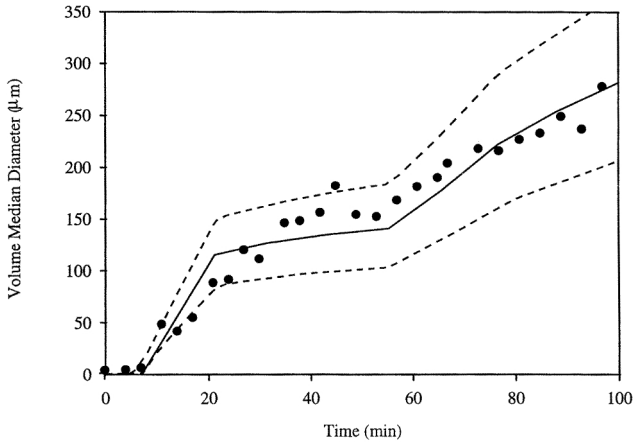

Figure 11. Use of model under different process (and thus agglomeration) conditions with 50% confidence intervals for model predictions.

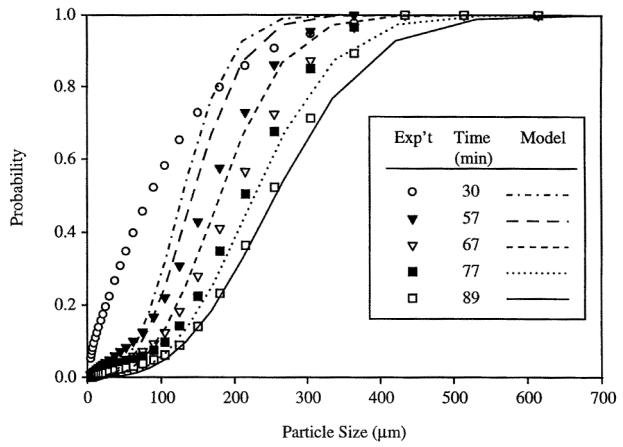

Figure 12. Particle-size distribution comparison between model predictions and pilot-plant observations.

successfully predict multiple regimes of rapid growth under diverse conditions.

Figure 12 represents the measured and predicted particle-size distribution throughout the experimental run for VMD results given by Figure 11. The DPB system overestimates the lower end of the particle-size distribution early in the granulation process, indicating that a more complex coalescence kernel and/or mechanism is governing the coalescence process. However, modeling of the agglomeration process using a DPB with the proposed three-parameter Stokes number kernel at later times (when the particle-size distribution is of industrial importance) is adequate to address optimization and sensitivity analysis questions.

Conclusions

Dow AgroSciences currently utilizes fluid beds for formulating active ingredients (solid powders) into water dispersible granules (or agglomerates). A mathematical model is formulated and solved utilizing recent research advancements in the area of population modeling and stochastic response surfaces.

A discretized population balance is used to describe the coalescence process in agglomeration. Uncertainty is characterized by the deterministic equivalent modeling method. A new mechanistic coalescence kernel is proposed. This kernel is simpler than previous researchers postulating size-independent coalescence kernels (that is, less empirical parameters) yet provides accurate descriptions for the physics involved under uncertainty. In addition, this kernel is capable of predicting experimental observations. The proposed coalescence kernel is an indirect function of process variables specific for fluid beds through the coupling with the Stokes number methodology.

Current simulations using the model outlined in this article suggest that pilot-plant fluid-bed observations can be adequately simulated for granule sizes of industrial importance. A definitive program is currently under way consisting of a statistical experimental design for isolation of major process variables and for providing data sets which can be used for model validation. Comparison between model predictions and experimental observations will yield estimates for the critical Stokes number. Once the critical Stokes number (or function) is known for a specific type of process, the model can be used for scale-up under a variety of different operating regimes and/or bed geometries. Extrapolation to the manufacturing scale fluid-bed agglomerator is anticipated.

Acknowledgments

The author wishes to recognize the Dow AgroSciences pilot-plant team, with special thanks to Ron Cassell and Marty Logan for both allowing and performing experimental runs on the pilot-scale fluid-bed granulator.

Literature Cited

Adetayo, A. A., and B. J. Ennis, "Unifying Approach to Modeling Granule Coalescence Mechanisms," *AIChE J.*, **43**, 927 (1997).

Adetayo, A. A., J. D. Lister, S. E. Pratsinis, and B. J. Ennis, "Population Balance Modeling of Drum Granulation of Materials with Wide Size Distribution," *Powder Technol.*, **82**, 37 (1995).

Barnocky, G., and R. H. Davis, "Elastohydrodynamic Collision and Rebound of Spheres—Experimental Verification," *Physics of Fluids*, **31**, 1324 (1988).

Dafniotis, P., and W. Ray, "Numerical Methods for Emulsion Copolymerization Reactor Models with Particle Aggregation," AIChE Annual Meeting, Chicago (Nov. 10–15, 1996).

Davidson, J. F., and D. Harrison, *Fluidized Particles*, Cambridge Univ. Press, New York (1963).

Ennis, B. J., J. Li, G. I. Tardos, and R. Pfeffer, "The Influence of Viscosity on the Strength of an Axially Strained Pendular Liquid Bridge," *Chem. Eng. Sci.*, **45**, 307 (1990).

Ennis, B. J., G. T. Tardos, and R. Pfeffer, "A Microlevel-Based Characterization of Granulation Phenomena," *Powder Technol.*, **65**, 257 (1991).

Ennis, B. J., and J. D. Lister, "Size Enlargement," *Perry's Chemical Engineer's Handbook*, 7th ed., Section 8, McGraw-Hill, New York (1997).

Ghanem, R. G., and P. D. Spanos, *Stochastic Finite Elements: A Spectral Approach*, Springer-Verlag, New York (1991).

Golovin, A. M., *Sov. Phys. Dokl.*, **8**, 191 (1963).

Hounslow, M. J., R. L. Ryall, and V. R. Marshall, "A Discretized Population Balance for Nucleation, Growth, and Aggregation," *AIChE J.*, **34**, 1821 (1988).

Kapur, P. C., and D. W. Fuerstenau, "Coalescence Model for Granulation," *Ind. Eng. Chem. Process Des. Dev.*, **8**, 56 (1969).

Kapur, P. C., "Kinetics of Granulation by Nonrandom Coalescence Mechansm," *Chem. Eng. Sci.*, **27**, 1863 (1972).

Kunii, D., and O. Levenspiel, *Fluidization Engineering*, 2nd ed., Series in Chemical Engineering, Butterworth-Heinemann, Newton, MA, (1991).

Lister, J. D., D. J. Smit, and M. J. Hounslow, "Adjustable Discretized Population Balance for Growth and Aggregation," *AIChE J.*, **41**, 591 (1995).

Mori, S., and C. Y. Wen, "Estimation of Bubble Diameter in Gaseous Fluidized Beds," *AIChE J.*, **21**, 109 (1975).

Sastry, K. V. S., "Similarity Size Distribution of Agglomerates During Their Growth by Coalscence in Granulation or Green Pelletization," *Int. J. Min. Proc.*, **2**, 187 (1975).

Tatang, M. A., "Direct Incorporation of Uncertainty in Chemical and Environmental Engineering Systems," PhD Thesis, MIT, Cambridge, MA (1995).

Tardos, G., *Proc. Annu. Fine Particles Society Meeting*, Fine Particles Society, Chicago (1995).

Werther, J., "Effect of Gas Distribution on the Hydrodynamics of Gas Fluidized Beds," *Ger. Chem. Eng.*, **1**, 166 (1978).

Manuscript received Dec. 7, 1998, and revision received June 18, 1999.